CHINESE OPTICS LETTERS

Vol. 20, No. 1 | January 2022

Passive patterned polymer dispersed liquid crystal transparent display

Jing Yan (严 静)[1,2*], Xiangwen Fan (范相文)[1], Yifan Liu (刘一帆)[3], Ying Yu (于 映)[1,2], Yuming Fang (方玉明)[1,2], and Ruo-Zhou Li (李若舟)[1,2**]

[1] College of Electronic and Optical Engineering & College of Microelectronics, Nanjing University of Posts and Telecommunications, Nanjing 210023, China

[2] National and Local Joint Engineering Laboratory of RF Integration and Micro-Assembly Technology, Nanjing University of Posts and Telecommunications, Nanjing 210023, China

[3] Touch and Display Module Development Group, Microsoft Inc., Suzhou 215123, China

*Corresponding author: jing.yan@njupt.edu.cn

**Corresponding author: lirz@njupt.edu.cn

Received July 25, 2021 | Accepted July 30, 2021 | Posted Online September 28, 2021

A patterned polymer dispersed liquid crystal transparent display using one-time UV exposure is demonstrated. The device is fabricated by exposing the cell with a uniform UV light through a mask with selective attenuation of the UV light. The voltage-transmittance response of the device is different for the corresponding regions. Thus, three different states of total scattering, patterned transparent, and total transparent can be realized by controlling the applied voltages. The proposed device used in shutter mode as smart windows and in projected display mode is demonstrated, which shows great potential for smart windows with customized patterns or logos and has potential application in the field of projected transparent displays.

Keywords: polymer dispersed liquid crystal; transparent display.

DOI: 10.3788/COL202220.013301

1. Introduction

Transparent displays are favored as next-generation display devices with the characteristics of rendering images on the panel, and the observers can see the scenery from both sides at the same time[1]. It is widely used in various scenes, such as smart windows, head-up displays, near-eye displays, and advertising[2–6]. Transparent displays have been developed in various ways. One type is active transparent display, such as transparent active matrix organic light-emitting diode (AMOLED) displays[7,8], active-matrix transparent display using polymer dispersed liquid crystal (PDLC) or electrochromic materials[1,9,10]. AMOLED transparent display usually has a light-emitting area and a transparent area. The two areas are arranged to form a periodic structure. The device appears transparent at a voltage-off state. As voltage is applied to the pixel, the light-emitting area displays images, and the other area maintains transparency. Active PDLC or electrochromic displays utilize the electric field to control the display mode of each pixel to convert between the transparent state and display state. Another class is passive transparent display, which requires a projection display to project an image onto a specific screen. A transparent medium embedded with nanoparticles can be used as the aforementioned screen to selectively scatter light at the projected wavelength, and the non-projected area maintains transparency[11]. Electrically switchable PDLC is also widely utilized as the projection screen or smart windows with scattering and transparent states due to its polarization independence, simple fabrication, and low cost for large-area displays[12–21]. Wu's group used the principle where PDLC film is highly transparent for a wide range of incident angles in the air but strongly scattering at large oblique angles in the high refractive index medium to realize a dual-plane see-through near-to-eye display[12]. Kim *et al.* developed PDLC-based large-area flexible smart windows using roll-to-roll slot die coating with Ag nanowire electrodes[22]. Besides, PDLC used to define the projected image shape in a see-through projected display device was proposed by Su *et al.*[23]. Last but not least, Wang's group proposed an integral imaging-based 2D/3D convertible display system by using holographic optical elements and PDLC film[24].

In this Letter, we propose a patterned PDLC transparent display using one-time UV exposure. The device is fabricated by exposing the cell with a uniform UV light through a patterned mask, which selectively attenuates the UV light. The patterned UV light causes patterned polymer concentration of the PDLC, resulting in different voltage-transmittance responses of the device for different regions. Thus, three different states of total

scattering, patterned transparent, and total transparent can be realized by applying proper driving voltages, respectively.

2. Fabrication and Working Principle

Figure 1 illustrates the fabrication process of a patterned PDLC transparent display. The PDLC employed in this Letter is a mixture composed of 60% (mass fraction) liquid crystal E7 (HCCH) and 40% (mass fraction) monomer NOA65 (Norland). The precursor in the isotropic state (~60°C) is injected into a 20 μm cell made with two indium tin oxide (ITO) substrates. A 4 mm × 4 mm mask with 82.5% UV attenuation is attached on the top substrate of the cell, as shown in Fig. 1(a). The cell was cured by a uniform UV lamp (365 nm, JZ40, Suzhou Jingzhen Photoelectric Technology Co., Ltd.) for 30 min, as Fig. 1(b) shows. Thus, a patterned UV exposure dosage distribution is obtained through the mask. The UV light intensities for region A and region B are 1.45 mW/cm^2 and 8.3 mW/cm^2, respectively. After UV curing, the attached mask is peeled off, and the patterned PDLC transparent display is obtained.

The electro-optical property of PDLC film is determined by the PDLC droplet size. Higher UV intensity results in smaller droplets and higher threshold voltage, while lower UV intensity leads to larger droplets and lower threshold voltage[25,26]. Thus, a patterned polymer concentration of PDLC film for transparent displays or smart windows is obtained by the preparation process above, and the pattern is determined by the customized mask with selective attenuation of the UV light. The working principle of the proposed device is shown in Fig. 2. The precursor in central area A is cured by the lower intensity of UV light; thus, the droplet size in region A is significantly larger than that in region B. At the voltage-off state, the cured PDLC film in both region A and region B scatters incident light because of the mismatched refractive indices of the liquid crystal and the polymer, as Fig. 2(a) shows. In other words, the proposed device presents

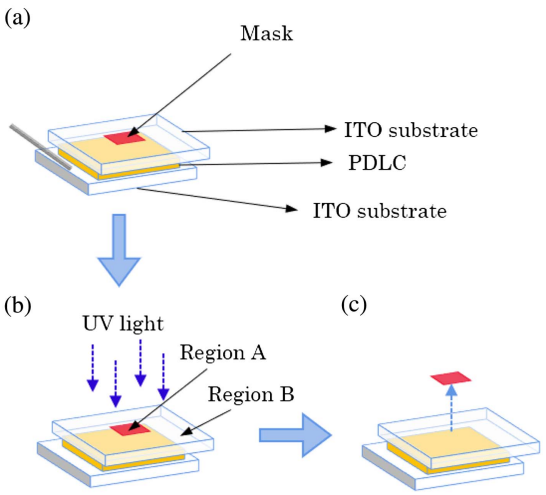

Fig. 1. Fabrication process of the patterned PDLC transparent display. (a) Injecting the PDLC precursor. (b) UV exposure. (c) Peeling off the mask.

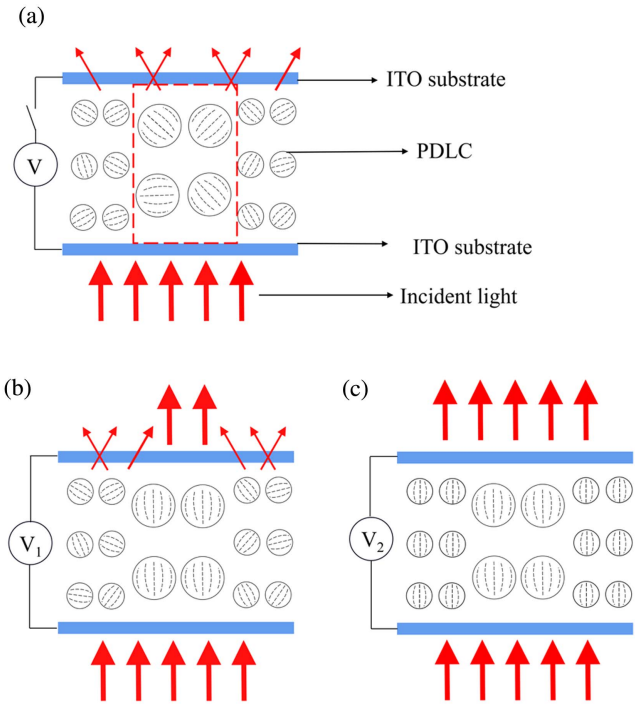

Fig. 2. Working principle of the patterned PDLC transparent display. (a) Voltage-off state. (b) Voltage-on state with V_1. (c) Voltage-on state with V_2 and $V_2 > V_1$.

a total scattering state. When a low voltage V_1 is applied between the ITO electrodes, a uniform electric field is applied to the sample. The PDLC in region A becomes transparent, while the PDLC in region B still stays in scattering mode because of its higher threshold voltage due to smaller droplet size, achieving the patterned transparent mode, as shown in Fig. 2(b). As the applied voltage increases to V_2, which is greater than the threshold voltage of PDLC in region B, all liquid crystal molecules in the device are aligned parallel to the electric field, all the incident light will go through without scattering, and the total transparent mode is obtained, as shown in Fig. 2(c).

3. Results and Discussions

To investigate the electro-optical properties of the two regions, we measure the voltage-transmittance curves (V-T curves) of region A and region B. The device is driven by a square-wave voltage signal of 1 kHz in frequency, and the transmitted light intensity through the device is received by a photodetector (New Focus 2031) and recorded by an oscilloscope (Tektronix TBS1102X). The blue square dotted line represents the measured V-T curve of the PDLC in region A, while the red circle dotted line indicates the measured data for region B in Fig. 3(a). It is clearly shown that the cured PDLC in region A has a lower threshold voltage of 16.04V_{rms} than that in region B (21.26 V_{rms}). The transmittance of region A dramatically increases when the applied voltage rises beyond 16.04 V_{rms}, while region B still stays in the scattering mode with low

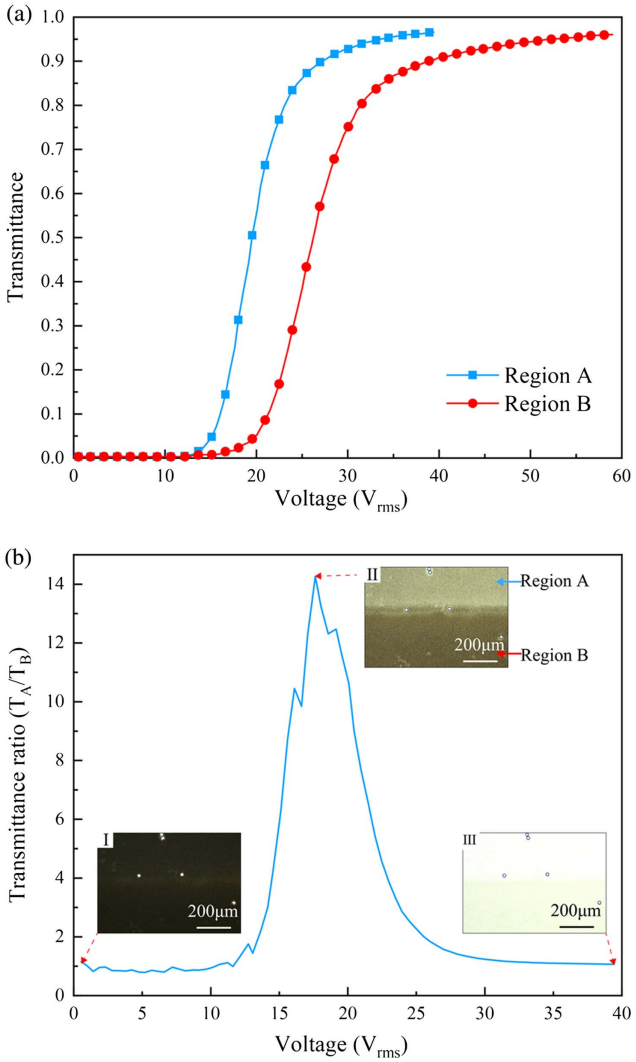

Fig. 3. (a) Measured *V-T* curves of region A and region B of the device. (b) The variation of the transmittance ratio of region A and region B with applied voltage. Insets: the morphologies of the two regions with different applied voltages under a microscope. (I) 0 V_{rms}; (II) 17.6 V_{rms}; (III) 40 V_{rms}.

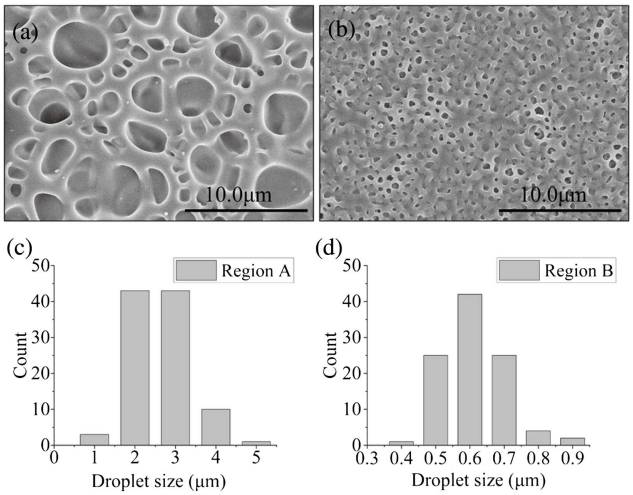

Fig. 4. SEM images of (a) region A and (b) region B. The droplet size distributions of (c) region A and (d) region B.

transmittance. When the applied voltage increases above 21.26 V_{rms}, region B starts to turn into the transmission mode, but still has a much lower transmittance than region A, which is almost totally transparent at that time. When the applied voltage increases over 31.53 V_{rms}, the transmittance of both region A and region B is larger than 0.80, resulting in the total transparent state for the proposed device.

The transmittance ratio of region A and region B (T_A/T_B) with applied voltage is calculated to quantitatively characterize the electro-optical property of the patterned PDLC transparent display at different driven voltages, as Fig. 3(b) shows. As the voltage increases from 0 V_{rms}, the transmittance ratio stays close to one, which indicates that both regions are in the scattering state. As the voltage continues to rise over 11.62 V_{rms}, there is a sharp increase in the transmittance ratio, and a maximum transmittance ratio of 14.26 is obtained at 17.63 V_{rms}. After that, the transmittance ratio decreases with the further increase of the voltage, as the high electric field makes the liquid crystal molecules in region B also reorient perpendicularly to the substrates, resulting in the transparent state for both regions. The morphologies of the two regions in the device are directly observed through a polarized optical microscope (Olympus BX-53) with parallel polarizers under different applied voltages of 0 V_{rms}, 17.6 V_{rms}, and 40 V_{rms}, as the insets show in Fig. 3(b). The boundary between the two regions is clearly visible, and the droplet morphology in region B is more compact and uniform. At the total scattering or total transparent states, there is no obvious contrast. A significant morphological difference is obtained at 17.6 V_{rms}. A large amount of light can pass through region A, while region B remains low transmittance. Figures 4(a) and 4(b) illustrate the SEM images of regions A and B. The average liquid crystal droplet sizes for the corresponding area are 2.65 μm and 0.62 μm, respectively. A lower UV light intensity results in a larger droplet size, leading to a lower threshold voltage.

Figure 5 demonstrates that the patterned PDLC transparent display can be used in shutter mode as a smart window. The photographs of the total scattering, patterned transparent, and total transparent modes of the device for the scenery far away and the graph nearby are shown in Figs. 5(a) and 5(b), respectively. At the voltage-off state, neither the scenery nor the graph can be seen through the device, due to the strong scattering of the device. As a 17.6 V_{rms} voltage is applied to the device, the scenery and the graph behind region A emerge, while behind region B they are still scattered. On the other hand, the device appears in the total transparent state when a larger voltage is applied, all of the scenery and graph behind the device can be seen clearly through the device. Thus, this proposed patterned PDLC transparent display can be used as smart windows with customizable patterns or logos, especially for translucent partition walls, public information displays, advertising, etc.

As the proposed device can operate in the scattering state or transparent state by controlling the applied voltage, the device

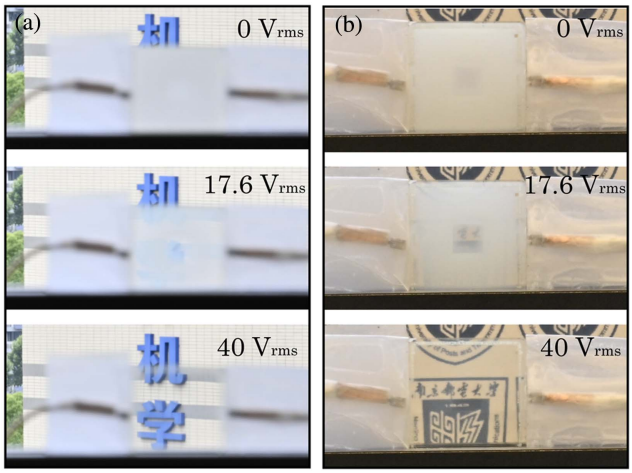

Fig. 5. Patterned PDLC transparent display is used in shutter mode as smart windows. (a) The display performance for the scenery in the distance. (b) The display performance for the graph nearby.

working in partial scattering mode or total scattering mode can also be used as a specific screen for the projected image. Figure 6 demonstrates the performance of the patterned transparent display in the projected display mode. A projector (LG PB63U) projects an image containing colorful geometric patterns and letters on the device and places a black card printed with a color pattern or a phone screen displayed with letters behind it. Although the projected image is more or less scattered, the image information can be still distinguished at the voltage-off state. The information behind the device cannot be seen in this case. Then, when a voltage of 17.6 V_{rms} is applied to switch the device to patterned transparent mode, the image behind region A can be seen, and the projected image including a yellow sun,

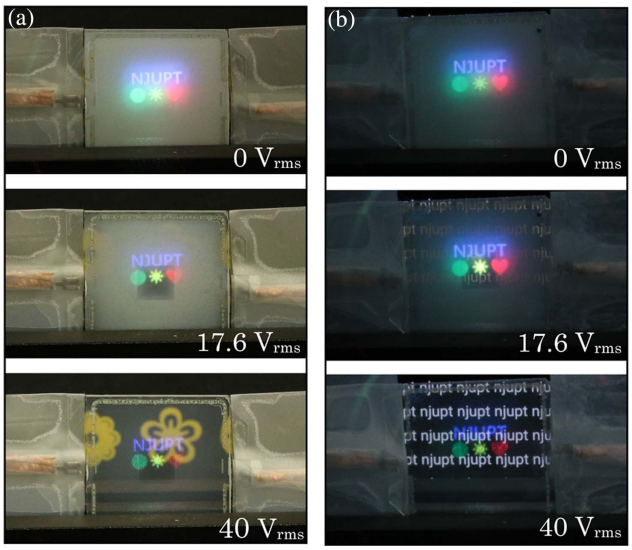

Fig. 6. Patterned PDLC transparent display is used in projected display mode. (a) A black card printed with a color pattern behind the device. (b) A phone screen displaying letters behind the device.

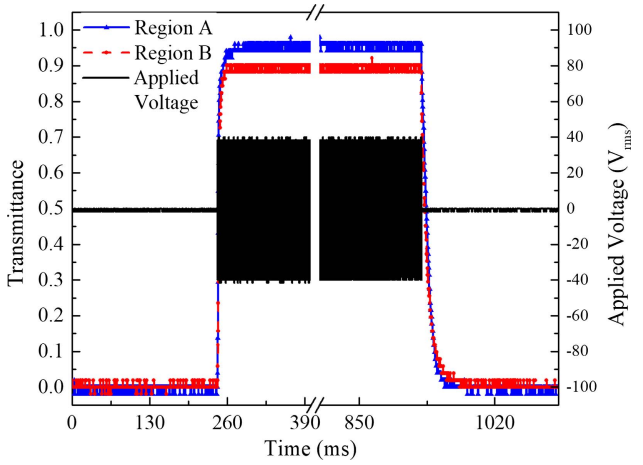

Fig. 7. Response time of region A and region B for the operating voltage of 40 V_{rms}.

a half-green circle, and a half-red heart is projected to the background black card or the phone screen. Meanwhile, the other half-green circle, the other half-red heart, and the blue letters "NJUPT" are still scattered. On the other hand, the phone screen has a brighter light, so the information behind region B is faintly visible, as Fig. 6(b) depicts. For the total transparent mode, the images behind the device are seen clearly, and the projected information is shown on the background image at the same time.

The response time of the proposed device is also measured for the different regions, as shown in Fig. 7. The blue triangle line and red square dashed line represent the transmittance of region A and region B, and the black line stands for the operating voltage of 40 V_{rms}. The rise and decay times are those associated with transmittance changes from 10% to 90% and from 90% to 10%, respectively. The rise time and decay time for region A are 4.96 ms and 15.62 ms, while those are 5.58 ms and 17.67 ms for region B. This response speed meets the requirements of smart windows and transparent displays. Moreover, the overdrive and undershoot method can also be introduced to further improve the response time[27].

4. Conclusion

In conclusion, a patterned PDLC transparent display using one-time UV exposure is proposed. The patterned intensity distribution of UV light is achieved by exposing the device through an attached mask with a selective attenuation pattern, leading to the patterned polymer concentration of the PDLC. The voltage-transmittance response of the device for region A and region B is quite different in turn. Thus, three different states of total scattering, patterned transparent, and total transparent can be realized. The patterned PDLC transparent display used in shutter mode as smart windows and in projected display mode is demonstrated. This patterned PDLC transparent display can be optimized for smart windows with customized patterns or logos and

potential applications in the field of projected transparent displays.

Acknowledgement

This work was supported by the National Natural Science Foundation of China (Nos. 11904177 and 61704090) and the Natural Science Foundation of Jiangsu Province (Nos. BK20170908 and BK20170903).

References

1. C.-W. Su and M.-Y. Chen, "Polymer-dispersed liquid crystal applied in active-matrix transparent display," J. Disp. Technol. **10**, 683 (2014).
2. C.-W. Chen, A. N. Brigeman, T.-J. Ho, and I. C. Khoo, "Normally transparent smart window based on electrically induced instability in dielectrically negative cholesteric liquid crystal," Opt. Mater. Express. **8**, 691 (2018).
3. H. Peng, D. Cheng, J. Han, C. Xu, W. Song, L. Ha, J. Yang, Q. Hu, and Y. Wang, "Design and fabrication of a holographic head-up display with asymmetric field of view," Appl. Opt. **53**, H177 (2014).
4. K. Akşit, W. Lopes, J. Kim, P. Shirley, and D. Luebke, "Near-eye varifocal augmented reality display using see-through screens," ACM Trans. Graphic. **36**, 1 (2017).
5. Z. Chen, X. Sang, H. Li, Y. Wang, and L. Zhao, "Ultra-lightweight and wide field of view augmented reality virtual retina display based on optical fiber projector and volume holographic lens," Chin. Opt. Lett. **17**, 090901 (2019).
6. S. Ikawa, N. Takada, H. Araki, H. Arali, H. Niwase, H. Sannomiya, H. Nakayama, M. Oikawa, Y. Mori, T. Kakue, T. Shimobaba, and T. Ito, "Real-time color holographic video reconstruction using multiple-graphics processing unit cluster acceleration and three spatial light modulators," Chin. Opt. Lett. **18**, 010901 (2020).
7. J. Chung, J. Lee, J. Choi, C. Park, J. Ha, H. Chung, and S. S. Kim, "Transparent AMOLED display based on bottom emission structure," in *SID Symposium Digest of Technical Papers* (2010), p. 148.
8. M. S. Chan Il Park, M. A. Kim, D. Kim, H. Jung, M. Cho, S. H. Lee, H. Lee, S. Min, J. Kim, M. Kim, J.-H. Park, S. Kwon, B. Kim, S. J. Kim, W. Park, J.-Y. Yang, S. Yoon, and I. Kang, "World 1st large size 77-inch transparent flexible OLED display," in *SID Symposium Digest of Technical Papers* (2018), p. 710.
9. C.-W. Su, C.-C. Liao, and M.-Y. Chen, "Color transparent display using polymer-dispersed liquid crystal," J. Disp. Technol. **12**, 31 (2016).
10. J. W. Kim and J. M. Myoung, "Flexible and transparent electrochromic displays with simultaneously implementable subpixelated ion gel-based viologens by multiple patterning," Adv. Funct. Mater. **29**, 1908911 (2019).
11. C. W. Hsu, B. Zhen, W. Qiu, O. Shapira, B. G. DeLacy, J. D. Joannopoulos, and M. Soljacic, "Transparent displays enabled by resonant nanoparticle scattering," Nat. Commun. **5**, 3152 (2014).
12. Z. He, K. Yin, and S. T. Wu, "Passive polymer-dispersed liquid crystal enabled multi-focal plane displays," Opt. Express **28**, 15294 (2020).
13. M. Xu and H. Hua, "Geometrical-lightguide-based head-mounted lightfield displays using polymer-dispersed liquid-crystal films," Opt. Express **28**, 21165 (2020).
14. I. Abdulhalim, P. L. Madhuri, M. Diab, and T. Mokari, "Novel easy to fabricate liquid crystal composite with potential for electrically or thermally controlled transparency windows," Opt. Express **27**, 17387 (2019).
15. V. Sharma, P. Kumar, A. Sharma, C. Jaggi, and K. K. Raina, "Droplet configuration control with orange azo dichroic dye in polymer dispersed liquid crystal for advanced electro-optic characteristics," J. Mol. Liq. **233**, 122 (2017).
16. P. Kumar, V. Sharma, C. Jaggi, and K. K. Raina, "Dye-dependent studies on droplet pattern and electro-optic behaviour of polymer dispersed liquid crystal," Liquid Cryst. **44**, 757 (2017).
17. P. Kumar, V. Sharma, C. Jaggi, P. Malik, and K. K. Raina, "Orientational control of liquid crystal molecules via carbon nanotubes and dichroic dye in polymer dispersed liquid crystal," Liquid Cryst. **44**, 843 (2017).
18. L. De Sio, E. Ouskova, P. Lloyd, R. Vergara, N. Tabiryan, and T. J. Bunning, "Light-addressable liquid crystal polymer dispersed liquid crystal," Opt. Mater. Express **7**, 1581 (2017).
19. M. H. Saeed, S. Zhang, M. Yu, L. Zhou, J. Huang, Q. Feng, H. Lin, X. Wang, J. Hu, L. Zhang, and H. Yang, "Effects of oxygen heterocyclic acrylate monomers on the morphologies and electro-optical properties of polymer dispersed liquid crystal composite films," Optik **229**, 166254 (2021).
20. H. Jiang, W. Cai, K. Li, M. Cheng, V. Kumar, Z. Yin, D. Gérard, D. Luo, Q. Mu, and Y. Liu, "Holographically fabricated, highly reflective nanoporous polymeric distributed Bragg reflectors with red, green, and blue colors," Chin. Opt. Lett. **18**, 080007 (2020).
21. Z. Diao, L. Kong, J. Yan, J. Guo, X. Liu, L. Xuan, and L. Yu, "Electrically tunable holographic waveguide display based on holographic polymer dispersed liquid crystal grating," Chin. Opt. Lett. **17**, 012301 (2019).
22. D.-J. Kim, D. Y. Hwang, J.-Y. Park, and H.-K. Kim, "Liquid crystal-based flexible smart windows on roll-to-roll slot die-coated Ag nanowire network films," J. Alloy. Compd. **765**, 1090 (2018).
23. S.-L. Hou, W.-K. Choi, and G.-D. Su, "High efficient polymer dispersed liquid crystal for ultra-bright projected image," Proc. SPIE **8828**, 882816 (2013).
24. H. L. Zhang, H. Deng, J. J. Li, M. Y. He, D. H. Li, and Q. H. Wang, "Integral imaging-based 2D/3D convertible display system by using holographic optical element and polymer dispersed liquid crystal," Opt. Lett. **44**, 387 (2019).
25. F. Ahmad, M. Jamil, J. W. Lee, S. R. Kim, and Y. J. Jeon, "The effect of UV intensities and curing time on polymer dispersed liquid crystal (PDLC) display: a detailed analysis study," Electron. Mater. Lett. **12**, 685 (2016).
26. Y. Liu, S. Xu, D. Xu, J. Yan, Y. Gao, and S.-T. Wu, "A hysteresis-free polymer-stabilised blue-phase liquid crystal," Liquid Cryst. **41**, 1339 (2014).
27. D. K. Yang and S. T. Wu, *Fundamentals of Liquid Crystal Devices*, 2nd ed. (Wiley, 2014).